Diode-side-pumped AO Q-switched Tm,Ho:LuLF laser

Shijiang Shu (舒仕江)[1,2], Ting Yu (余 婷)[1,2*], Rongtao Liu (刘荣涛)[1,2], Junyan Hou (侯军燕)[3], Xia Hou (侯 霞)[1,2], and Weibiao Chen (陈卫标)[1,2]**

[1]*Shanghai Key Laboratory of All Solid-State Laser and Applied Techniques, Shanghai Institute of Optics and Fine Mechanics, Chinese Academy of Sciences, Shanghai 201800, China*

2*Research Center of Space Laser Information Technology, Shanghai Institute of Optics and Fine Mechanics, Chinese Academy of Sciences, Shanghai 201800, China*

[3]*Beijing Institute of Tracking and Telecommunication Technology, Beijing 100094, China*

[*]*Corresponding author: yuting@mail.siom.ac.cn;* [**]*corresponding author: wbchen@mail.shcnc.ac.cn*

Received February 21, 2011; accepted April 21, 2011 ; posted online July 11, 2011

A diode-side-pumped Tm,Ho:LuLiF laser at 2-μm wavelength obtained in a ring resonator and its amplification experiment are reported. At the maximum pump energy of 4.7 J available for the oscillator, the output energy per pulse for the oscillator decreases from 904 to 483 mJ in free running mode, and decreases from 106 to 68 mJ in Q-switched mode, with an increase of pump pulse repetition rate from 1 to 5 Hz. When considering the amplifier, 99-mJ Q-switched output energy is achieved at 5-Hz repetition rate.

OCIS codes: 140.0140, 140.3540, 140.3580.
doi: 10.3788/COL201109.091407.

The development of solid-state lasers in the 2-μm region has received considerable attention because of the various potential applications of the lasers in altimetry, ranging, and atmospheric remote sensing, including wind sensing by Doppler lidars and CO_2 profiling by differential absorption lidars (DIALs). Among these applications, coherent Doppler wind lidars and CO_2 DIALs at eye-safe 2-μm spectral range can provide tropospheric wind profiles and CO_2 vertical profiles, respectively, with high measurement precision[1−5]. The key component in these lidar systems is a reliable, high pulse energy, and single frequency laser. Developing this kind of transmitter profits from the appearance of all kinds of solid-state 2-μm laser active media. These media are typically doped with Tm^{3+} or Ho^{3+} or co-doped with Tm^{3+} and Ho^{3+}. The Ho $^5I_7$–$^5I_8$ transition has a markedly higher lasing emission cross section than the Tm $^3F_4$–$^3H_6$ transition. However, Ho does not possess an absorption band to match the emission of commercially available laser diodes. This leads to the Ho^{3+} co-doping with Tm^{3+}. In the co-doped media, Tm^{3+} acts as sensitizer to transfer the absorbed pumping energy into a Ho^{3+} metastable energy state efficiently.

Among these active media co-doped with Tm^{3+} and Ho^{3+}, Tm,Ho:LuLF has performed better compared to other similar laser crystals at a low pulse repetition rate[6−13]. In 2004, a joule-level 2-μm laser master oscillstor power amplifier (MOPA) system operated in double-pulse format was reported[14]. Two years later, the system was improved and a 1-J/pulse Q-switched output was obtained[15]. This fact proves that Tm,Ho:LuLF has its own advantage in terms of obtaining a large pulse energy. To construct a coherent Doppler wind lidar system, a high-energy laser transmitter based on Tm,Ho:LuLF is being developed in our laboratories[16−19]. In this letter, we report the performance of the transmitter's oscillator and amplifier.

The whole experimental setup comprises an oscillator and an amplifier (Fig. 1). A ring resonator configuration is used to avoid spatial hole burning because the final application requires a narrow linewidth output. The resonator consists of two curved high reflectors, one flat reflector, and one flat output coupler (O.C.). An O.C. with 70% reflectivity is used as a compromise between the output energy and the fluence inside the resonator. M1, M4, and M5 are high-reflectivity flat mirrors. M2 and M3 are curved mirrors with a 4-m radius of curvature. The two curved high reflectors make two Gaussian beam waists inside the cavity. The laser crystal rod and an anti-reflection(AR)-coated crystal quartz acousto-optical (AO) Q-switch are located at these two Gaussian beam waists. In this experiment, M4 is used to obtain unidirectional output. The total resonator length for this laser is approximately 2 m.

The Tm,Ho:LuLF laser rod is cut along the a-axis with 5% Tm and 0.5% Ho concentration. Its dimension is 4 mm in diameter and 23 mm in length. The rod ends are AR-coated for the emission wavelength of 2-μm. Two brass caps are bonded to the rod ends for seal and support. Since the laser emits π-polarization light and the Q-switch used in the experiment is a polarization-dependent device, the laser rod should be rotated along its axis to make its c-axis match with the Q-switch for a higher hold-off capacity. In this experiment, the c-axis of the laser rod is adapted to be vertical to the experimental platform.

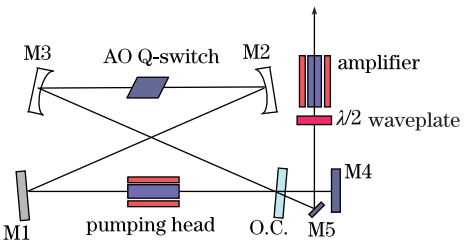

Fig. 1. Schematic diagram of the experimental setup.

The pumping heads in the oscillator and the amplifier have the same structure and parameters (Fig. 2). The laser rod is encased in an 8-mm outer-diameter fused-silica glass tube for water cooling. The coolant temperature is set at 10 °C. Three AlGaAs laser diode arrays are located 120° apart around the circumference of the rod. Each diode array has 15 bars 1 cm in length. The individual array can provide pump radiation of up to 1.7 J at around 792 nm with 1-ms pulse width. The diode arrays are directly mounted on stainless steel modules and cooled by flowing water at 25 °C. The pump diode arrays and the laser crystal rod are cooled in different loops, so the temperatures of the diodes and the rod can be independently controlled. The cylinder lens between diode arrays and laser rod are applied to shape the divergent beams from these diode arrays and thus make full use of the pump energy. Finally, the area about 20 mm in length on the side of the rod is pumped by the diode arrays.

For the free running mode, the Q-switch inside the laser resonator is not activated. For the Q-switched mode, the laser is Q-switched once during one pump period. In the experiment, the pump pulse duration is set to be 1 ms. The population of the Ho upper laser manifold $^5I_7$ increases continuously during the pump duration, but does not reach the maximum at the end of the pump pulse. The Ho needs more time to acquire the energy transferred from the Tm $^3F_4$ manifold and thus reach its maximum after the end of the pump pulses. To maximize the output pulse energy, the Q-switched pulse should be triggered at the time when the $^5I_7$ population reaches its maximum value. The delay time is determined to be 92 μs in the experiment.

The results of the oscillator performance in both modes at different pump repetition rates are depicted in Figs. 3 and 4, respectively. At 1-Hz repetition rate, 904-mJ normal in free running mode and 106-mJ Q-switched

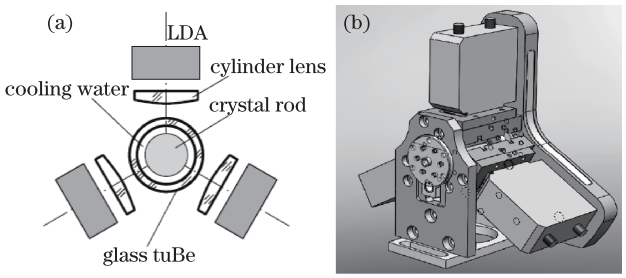

Fig. 2. Water-cooled laser head assembly. (a) Schematic diagram; (b) assembly drawing.

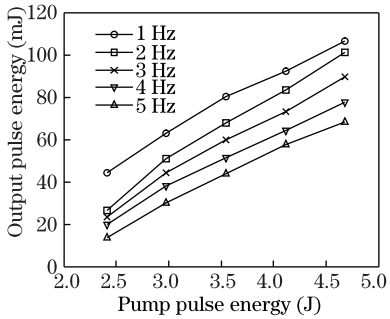

Fig. 3. Oscillator output performance for Q-switched mode at different repetition rates.

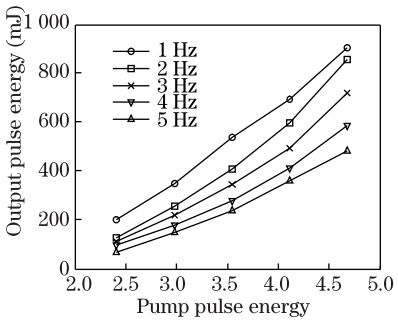

Fig. 4. Oscillator output performance for free running mode at different repetition rates.

output output in Q-switched mode are obtained for an input energy of 4.65 J, which correspond to the optical-to-optical efficiencies of 19.4% and 2.3%, respectively. At 5-Hz repetition rate, the normal pulse energy and the Q-switched pulse energy decrease to 483 and 68 mJ, respectively, and the corresponding optical-to-optical efficiencies decrease to 10.4% and 1.5%, respectively. The low efficiency at higher repetition rate can mainly be attributed to the increase of heat load on the rod. The increased heat load can affect the population inversion significantly because the Tm,Ho:LuLF laser at the 2-μm wavelength region belongs to a quasi-four-level laser. A lower temperature of the laser gain medium favors a decrease in threshold and an increase in efficiency. However, the temperature cannot be reduced further in the experiment because of the dew point constraint.

Figure 5 shows one of the Q-switched pulse waveforms. More than one mode oscillates in the resonator; hence, there is a mode beating superimposed on the pulse waveform. The long pulse obtained in free running mode

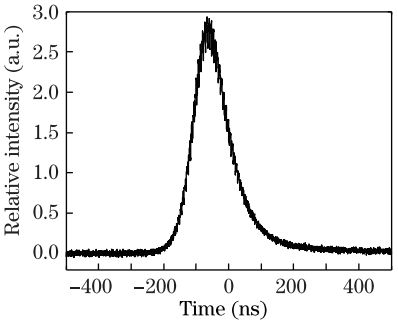

Fig. 5. Oscilloscope waveform of Q-switched pulse.

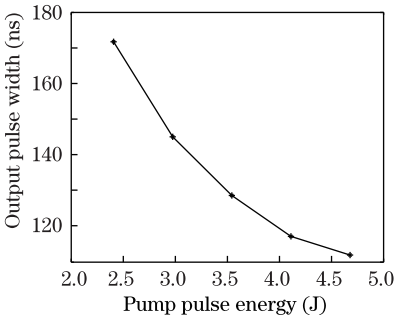

Fig. 6. Dependence of Q-switched pulse width on the pump energy at 5-Hz repetition rate.

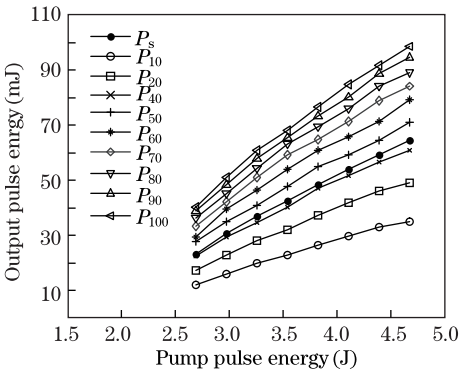

Fig. 7. Laser amplification experimental results for Q-switched mode at 5-Hz repetition rate.

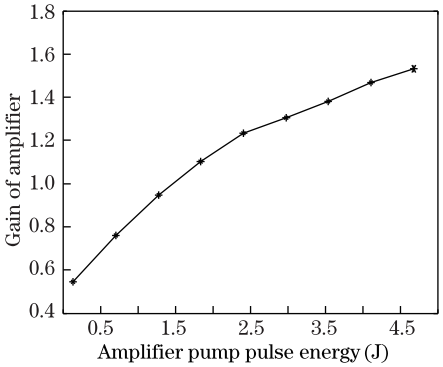

Fig. 8. Single-pass gain for amplifier.

typically has a width of several hundred microseconds for a pump pulse duration of 1 ms. The Q-switched pulse width at 5-Hz repetition rate is shown as a function of pump energy in Fig. 6. As the pump energy increases, the pulse width decreases, though it is still larger than the 100-ns pulse width required for a coherent wind lidar transmitter.

When considering the amplification experiment, M2 and M3 are replaced by two curved mirrors with a 4.5-m radius of curvature for a larger laser beam size, while M1 is replaced by a coupler with a transmittance of 5% for future signal detection. The laser beam out of the oscillator is reflected by M5 and then travels through the amplifying rod. Since the rod is anisotropic, a half-wave plate is needed to adjust the polarization direction of the laser beam before it enters the rod for the best amplification performance. The amplifier module and oscillator module are activated at the same time. Figure 7 shows the amplification experimental results for Q-switched mode at 5-Hz repetition rate.

In Fig. 7, the curve labeled P_s represents the output pulse energy of the oscillator without amplifier. Other curves represent the output pulse energy after amplification at the corresponding pump electric current of the amplifier, e.g., P_{20} represents the pump electric current of the amplifier at 20 A. According to Fig. 7, the amplifying rod demonstrates a positive net gain only above the pump electric current of ~40 A. Figure 8 shows the optical gain of the amplifier at 64 mJ of input energy. A 1.53 gain is obtained at the maximum pump power for the amplifier.

The low efficiency of the system is mainly due to the following factors. The two ends of the laser rod that is not pumped is considered to bring a net loss for the 2-μm laser. The side surface of the rod used in the experiment is frosted, so the diffused reflection prevents the pump beams from entering; only a part of the pump beams are absorbed because they pass the cross section of the rod just once. A feasible solution to improve the efficiency is by substituting a diffusion bonded rod for the one currently used.

In conclusion, a diode-side-pumped AO Q-switched 2-μm MOPA system is reported. The oscillator of the system can provide up to 106 and 68 mJ of Q-switched pulse energy at 1 and 5 Hz repetition rate, respectively. At these two repetition rates, the optical-to-optical conversion efficiencies are 2.3% and 1.5%, respectively. For a total system pump energy of ~9.3 J, 99-mJ Q-switched output energy is achieved at 5-Hz repetition rate. To obtain single frequency output, an injection seeding is required.

References

1. T. M. Taczak and D. K. Killinger, Appl. Opt. **37,** 8460 (1998).
2. M. J. Kavaya, G. D. Spiers, E. S. Lobl, J. Rothermel, and V. W. Keller, SPIE **2214,** 237 (1998).
3. M. J. Kavaya and G. D. Emmitt, Proc. SPIE **3380,** 2 (1998).
4. G. J. Koch, B. W. Barnes, M. Petros, J. Y. Beyon, F. Amzajerdian, J. Yu, R. E. Davis, S. Ismail, S. Vay, M. J. Kavaya, and U. N. Singh, Appl. Opt. **43,** 5092 (2004).
5. G. J. Koch, J. Y. Beyon, B. W. Barnes, M. Petros, J. Yu, F. Amzajerdian, M. J. Kavaya, and U. N. Singh, Opt. Eng. **46,** 116201 (2007).
6. E. D. Filer, C. A. Morrison, N. P. Barnes, and B. M. Walsh, in *Advanced Solid-State Lasers* (OSA) **20,** 127 (1994).
7. M. G. Jani, N. P. Barnes, K. E. Murray, D. W. Hart, G. J. Quarles, and V. K. Castillo, IEEE J. Quantum Electron. **33,** 112 (1997).
8. A. Bensalah, K. Shimamura, V. Sudesh, H. Sato, K. Ito, and T. Fukuda, J. Crystal Growth **223,** 539 (2001).
9. V. Sudesh, K. Asai, K. Shimamura, and T. Fukuda, Opt. Lett. **26,** 1675 (2001).
10. V. Sudesh, K. Asai, K. Shimamura, and T. Fukuda, IEEE J. Quantum Electron. **38,** 1102 (2002).
11. B. M. Walsh, N. P. Barnes, J. Yu, and M. Petros, in *Advanced Solid-State Lasers* (OSA) **68,** 245 (2002).
12. V. Sudesh and K. Asai, J. Opt. Soc. Am. B **20,** 1829 (2003).
13. B. M. Walsh, N. P. Barnes, M. Petros, J. Yu, and U. N. Singh, J. Appl. Phys. **95,** 3255 (2004).
14. S. Chen, J. Yu, M. Petros, Y. Bai, U. N. Singh, and M. J. Kavaya, Proc. SPIE **5653,** 175 (2004).
15. J. Yu, B. C. Trieu, E. A. Modlin, U. N. Singh, M. J. Kavaya, S. Chen, Y. Bai, P. J. Petzar, and M. Petros, Opt. Lett. **31,** 462 (2006).
16. S. Shu, T. Yu, J. Hou, R. Liu, M. Huang, and W. Chen, Chin. Opt. Lett. **9,** 021401 (2011).
17. T. Yu, S. Shu, and W. Chen, Chin. Opt. Lett. **9,** 041407 (2011).
18. L. Qiao, X. Hou, and W Chen, Chinese J. Lasers (in Chinese) **36,** 1327 (2009).
19. L. Qiao, X. Hou, and W. Chen, Chinese J. Lasers (in Chinese) **36,** 1843 (2009).